Spin dynamics and the delocalization of hole quasiparticles

J. M. F. Gunn
Rutherford Appleton Laboratory, Chilton, Didcot, Oxon OX11 0QX, England

B. D. Simons
Cavendish Laboratory, Madingley Road, Cambridge CB3 0HE, England
(Received 10 January 1990)

Hole motion through a Heisenberg antiferromagnet is examined using a restricted set of spin configurations to describe the spin distortion around the hole. The hole induces spin singlets, *not* ferromagnetism at the (magnetic) Brillouin-zone boundary. An inherently many-particle band structure is found. Each band is associated with a different spin distortion around the hole. Most of the bands are found dispersionless, in agreement with photoemission data from the high-temperature superconducting cuprates.

I. INTRODUCTION

A first step in understanding the role of antiferromagnetism in the oxide superconductors is the characterize the quasiparticles that are formed when the parent compounds (e.g., La_2CuO_4) are doped with a dilute gas of holes. In this paper we provide such a characterization by calculating the correlated band structure (instead of one band there are 17) of the quasiparticles, and examining their wave functions, revealing the nature of the local spin distortion around the hole. The resulting information will be useful in constructing models of *interacting* quasiparticles to examine magnetic or superconducting instabilities.

The simplest model that captures some of the physics of the Cu-O planes is the "t-J" model,[1,2] which contains both mobile holes and a Heisenberg spin system. (The model may either be regarded as a canonically transformed Hubbard model[3] or as an effective model resulting from consideration of Cu and O sites explicitly[2,4].) The holes are implicitly coupled to the spins (since they are displaced as the holes move).

There are three levels of complexity of treatments of the t-J model. Firstly, the antiferromagnetism of the spins may be ignored, then the ground state is ferromagnetic, at least as a square lattice,[5] and the excitations were considered by Brinkman and Rice.[6] Secondly, the Ising part of the antiferromagnetic exchange may be incorporated so that antiferromagnetism remains (at low enough doping). A single hole becomes spin polaronic, extending over a region of divergent extent as the exchange constant tends to zero. From the investigation of a previous paper (Simons and Gunn[7]) the following picture of the hole quasiparticle in the Ising case emerged: The hole, displacing a "string" of spins behind it as it moves, yields a linear potential, confining it to its "initial site." The quasiparticle is localized around a particular site and there are excitations which increase the average length of "string." Trugman[8] demonstrated that there are special trajectories for the hole ("Trugman cycles") which allow the hole to move between neighboring sublattice sites, without leaving a string, yielding a rather small bandwidth for the hole (ca. 10% of the full bandwidth). Furthermore, it was demonstrated in our previous paper[7] that, as well as the excitations which change the arclength of string, there are additional excitations where spin configurations of the *same* string length were weighted with different phases. It was suggested that these states dominate the optical absorption.

Finally, the t-J model may be treated fully by adding the transverse (XY) coupling of the spins, giving the spin system its own dynamics and restoring rotational symmetry. Several works[9-13] have been published recently in this area, deriving the spectral weight of the quasiparticle Green's function and arguing that the resulting bandwidth was of order the exchange constant J. [Gros and Johnson found the bandwidth was $\sim t(J/t)^{(2/3)}$.] One difference between the treatments was the representation of the spin operators: Holstein-Primakoff bosons,[9] Schwinger bosons,[10] and fermions.[11]

Although the Green's-function treatments of inclusion of the spin dynamics are likely to give a good account of certain aspects of the hole motion, they do not readily provide the information that a wave function would provide, on the nature of the short-range distortion of the spin system. In this paper we provide such a complementary treatment, using a variational approach which displays the preferred spin configurations associated with the short-range distortion. It allows us to investigate the $\mathbf{k}$ dependence of this distortion and shows what remnants there are of the excited states of the Ising limit studied in the previous paper (Simons and Gunn[7]). The effect of spin dynamics on hole propagation has also been investigated variationally, choosing a spin-wave expansion to describe the background Néel order (Sachdev[14]).

The variational basis allows only spin flips (or spins displaced by the hole motion) a certain distance (≤ 2 lattice parameters) from the "quasiparticle position." This distance is large enough for the transverse coupling to yield a finite effective mass, but small enough that much

of the problem may be solved analytically *exactly*. In fact, starting with a basis set of 17 states, we are left with only a 4×4 secular equation to solve approximately. Recently, based on the same prescription of defining basis states by damaging the region of Néel order around a hole, Trugman[12] has used a larger basis of states to construct the Green's function for a hole in an antiferromagnet. However, the analysis relies on computation and as such does not provide an analytical description of many of the properties described here.

The plan of this paper is as follows: Section II introduces the variational basis set, Sec. III reduces the problem to 4×4 secular equation and comments on the nature of the other 13 bands, Sec. IV focuses on the lowest band and its wave functions, Sec. V examines the spin distortion and its $\mathbf{k}$ dependence, and finally we discuss and conclude in Sec. VI.

II. INCORPORATION OF SPIN DYNAMICS

In this section we introduce the variational basis tailored to answering the following questions: What is the short-range spin distortion around a hole? How does this affect the effective mass? Conversely, the basis will *not* allow a discussion of the long-range part of the spin distortion[15,16] and, as will become apparent, the long-wavelength spin waves.

The Hamiltonian we wish to consider is the t-J model (Anderson[17] and Zhang and Rice[2,18])

$$\mathcal{H}=-t\sum_{\langle ij\rangle\sigma}[(1-n_{i\bar{\sigma}})c^{\dagger}_{i\sigma}c_{j\sigma}(1-n_{j\bar{\sigma}})+\text{H.c.}]$$
$$+J\sum_{\langle ij\rangle}\left[S_i^zS_j^z+\frac{\alpha}{2}(S_i^+S_j^-+S_i^-S_j^+)\right]. \tag{2.1}$$

Here $\langle ij\rangle$ denotes near-neighbor sites on a square lattice. We have allowed the magnetic exchange to be anisotropic so that, for purposes of interpretation, we can turn off the spin dynamics by letting $\alpha\rightarrow0$, yielding an Ising model.

The variational basis is based on the Ising limit, where the spin distortion caused by the hole, at least for $J/t\gtrsim1$, is well understood. There, a hole placed in a Néel state becomes, to a first approximation, a localized quasiparticle.[7] The "trapping" potential arises from the increase of the exchange energy due to the hole's motion: as it moves the hole displaces spins from the Néel state, thereby increasing its energy—growing roughly linearly with the distance it has traveled. This "string" of displaced spins confines it to the vicinity of the site on which it was placed. (Here we neglect the effect of the special configurations investigated by Trugman,[8] which allows the hole to weakly delocalize. This effect will be insignificant in comparison to the effects of the transverse coupling that we will include.)

The transverse (to the direction of the sublattice magnetization) coupling of the spins allows a pair of displaced spins to flip, and hence regain their orientations in the Néel state. This provides a mechanism for the string of displaced spins to relax and hence for the quasiparticle to move. Of course, the process may occur in the reverse order, where the spin flip occurs first and the hole motion second. This picture suggests the variational basis that we will use: with each site we associate a set of states with string lengths of zero, one, and two lattice parameters. (This basis set should be sufficient if the string tension is not too weak; we will return to consider how realistic this is presently.) As the transverse coupling is increased the degeneracy of these states is lifted and they become bands of Bloch states. Physically, we may interpret this procedure as the variational basis allowing a description of the "internal structure" of the quasiparticle and the incorporation of the transverse coupling allowing mobility.

Throughout this paper we will assume that the background Néel order remains intact. Clearly this assumption is not valid when there is more than one quasiparticle, however, providing the hole experiences at least short-range Néel order (the doping is not too high), we may hope to determine the short-wavelength behavior of the hole quasiparticle.

To construct the basis explicitly, let us review a number of results from the previous paper. We showed that the configuration space for the hole trajectories is a Bethe lattice with each site corresponding to particular hole position and spin arrangement. The "generation number" of the lattice is the arc length of the trajectory. Since we are treating the limit of high string tension, the hole quasiparticles are well represented by including only the low generations of the lattice—as mentioned above, we choose to truncate after the second generation. This leads to a basis set of 17 states per site, corresponding to the Néel state with the hole sitting on the site and 16 disordered spin configurations generated by the hole moving up to two lattice parameters away. The truncated Bethe lattice forms a Cayley tree of depth two.

We may now see how this choice of basis set, while describing the short-range spin distortion adequately, cannot describe the long-range part. It does not include the possibility of displaced spins farther away than two sites and hence does not allow for spin fluctuations, due to the transverse coupling farther away either. Thus, spin waves and the long-range distortion are not handled well.

We denote the sites, on the tree, by their generation number, n, and a set of "sibling" numbers, $\{\mathbf{i}\}$, which determine which pattern of branches of the Cayley tree have to be followed to reach the site. The corresponding state is $|n,\{\mathbf{i}\}\rangle$. The generation numbers are chosen to be -1 on the central "site" of the tree, 0 for the strings of length one, and 1 on the outer generation. The actual assignation of a particular sibling number to each state of a given generation is arbitrary and it is not necessary to make a particular choice. The allowed values of the sibling numbers are $0\le i_n\le\xi_n^2-1$, where

$$\xi_n^2=\begin{cases}(Z-1), & n>0,\\ Z, & n=0,\\ 1, & n=-1.\end{cases} \tag{2.2}$$

To investigate the behavior of the quasiparticles with higher dimensionality we have incorporated a general

coordination number for the underlying lattice, $\mathcal{Z}$. For the case of a square planar lattice the coordination number is four.

In terms of this basis set, the Hamiltonian has three terms: hopping between different generations of the tree on a given site, the string tension "potential", and hopping between neighboring trees caused by the transverse coupling. (It should be noted that the transverse coupling has no other effects within the basis set that we have chosen.) It is easy to see that only states on a given sublattice are connected. Thus, we will restrict our treatment to one sublattice. Explicitly,

$$\mathcal{H}=-\sum_{n\langle|\mathbf{i}||\mathbf{j}|\rangle\mathbf{R}}^{0}(|n;\{\mathbf{i}\};\mathbf{R}\rangle\langle n+1;\{\mathbf{j}\};\mathbf{R}|+\text{H.c.})+\sum_{n|\mathbf{i}|\mathbf{R}}^{1}V_n|n;\{\mathbf{i}\};\mathbf{R}\rangle\langle n;\{\mathbf{i}\};\mathbf{R}|+\frac{\alpha\tau}{2}\sum_{|\mathbf{i}|\mathbf{R}}(|-1;\mathbf{R}+\{\mathbf{i}\}\rangle\langle 1;\{\mathbf{i}\};\mathbf{R}|+\text{H.c.})\ . \quad (2.3)$$

Here we have used the hopping integral as the unit of energy. The ratio J/t describes the relative strength of the trapping potential imposed by the Ising coupling of the spins, and we will refer to it when loosely talking of the "string tension," τ. The vector $\mathbf{R}$ denotes the position of the magnetic sublattice site (on the real lattice) to which the Cayley trees are attached. The potential, V_n due to the hole scrambling the spin configuration from the Néel state, is given by

$$V_n=\begin{cases}[(\mathcal{Z}-2)n+(\mathcal{Z}-1)]\dfrac{\tau}{2}, & n\geq 0\ ,\\ 0, & n=-1\ .\end{cases} \quad (2.4)$$

We see from the last term in (2.3) that the effect of the transverse coupling is to provide matrix elements between second generation sites on one tree and the origin of the neighboring tree. Given the translational invariance of the underlying lattice, we define Bloch states, formed from the Cayley tree states from each sublattice site, by the following;

$$|n;\{\mathbf{i}\};\mathbf{k}\rangle=\frac{1}{\sqrt{\mathcal{N}}}\sum_{\mathbf{R}}e^{i\mathbf{k}\cdot\mathbf{R}}|n;\{\mathbf{i}\};\mathbf{R}\rangle\ , \quad (2.5)$$

where the sum runs over all the sublattice sites. The total number of sublattice sites in the lattice is given by $\mathcal{N}$. Since only states on a given magnetic sublattice are connected, it is more natural to work in the magnetic Brillouin zone. Thus, let us define the new cell parameter, $\bar{a}=\sqrt{2}a$ and new coordinate axes in $\mathbf{k}$ space, $k_1=(k_x+k_y)/\sqrt{2}$ and $k_2=(k_y-k_x)/\sqrt{2}$. If we substitute (2.5) into (2.3) we see that the Hamiltonian becomes

$$\mathcal{H}=-\sum_{n\langle|\mathbf{i}|\mathbf{j}|\rangle\mathbf{k}}^{0}(|n;\{\mathbf{i}\};\mathbf{k}\rangle\langle n+1;\{\mathbf{j}\};\mathbf{k}|+\text{H.c.})+\sum_{n|\mathbf{i}|\mathbf{k}}^{1}V_n|n;\{\mathbf{i}\};\mathbf{k}\rangle\langle n;\{\mathbf{i}\};\mathbf{k}|+\frac{\alpha\tau}{2}\sum_{|\mathbf{i}|\mathbf{k}}(e^{-i\mathbf{k}\cdot|\mathbf{i}|}|-1;\mathbf{k}\rangle\langle 1;\{\mathbf{i}\};\mathbf{k}|+\text{H.c.})\ . \quad (2.6)$$

We may see immediately that the "internal" structure of the polaron is momentum dependent, due to the $\mathbf{k}$ dependence of the matrix elements coupling the states from different generations. In general, the degeneracies associated with the uncoupled Cayley trees are broken, although as we will see in the next section a substantial number of (less obvious) degeneracies occur.

III. SOLUTION

The eigenstates of the Hamiltonian (2.6) form bands, as expected from the translational invariance of the problem; however, the bands are not of a single-particle nature—as may be seen immediately by noting that there are 17 states per sublattice site. This abundance of bands is due to the necessity of describing the spin distortion as well as merely the hole position. Remarkably, only 4 of these bands disperse and it is the main aim of this section to comprehend why the other 13 bands remain flat.

A particularly concise representation of the secular determinant, associated with the band-structure calculations, is the graph of the Hamiltonian matrix shown in Fig. 1. (This is particularly valuable when dealing with such a large matrix.) There, each node in the graph corresponds to one state [in this case the Bloch states defined in (2.5)] and each link corresponds to a nonzero matrix element, between the states associated with the appropriate nodes, in the Hamiltonian. The nodes and links have energies associated with them, corresponding to the diagonal and off-diagonal elements of the Hamiltonian, respectively. Our diagonalization of the Hamiltonian will rely heavily on this description.

We will now introduce a simple result which will greatly aid the manipulation of the Hamiltonian into a tractable form. Consider the Hamiltonian associated with a very simple graph (we will refer to this as the "tight-binding star" or TBS): one "central" site coupled to M others, which are not coupled to each other. We denote the sites by m, with the central site being $m=0$. The energy of the central site may be different from that of the other sites, which are assumed to have the same energy. However, we allow the matrix elements that couple the

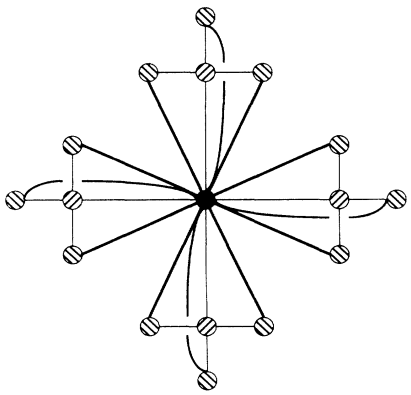

FIG. 1. The graph of connectivity of the Hamiltonian when expressed by means of the Bloch representation. Nodes with the same "on-site" energy are shaded in the same way. The bold lines indicate the momentum-dependent off-diagonal matrix elements.

central site to the others to be arbitrary, h_m. The Hamiltonian is

$$H_* = \varepsilon \sum_{m=1}^{M} |m\rangle\langle m| - \sum_{m=1}^{M} \{h_m |m\rangle\langle 0| + h_m^* |0\rangle\langle m|\} . \tag{3.1}$$

The eigenstates are of two types: those which have a nonzero amplitude at the central site (of which there are two), and those which do not (of which there are $M-1$). The eigenvalues of the first type, E^I, are determined by

$$\frac{\mathbf{h}^* \cdot \mathbf{h}}{E^I - \varepsilon} = E^I . \tag{3.2}$$

(Here we have defined a vector $\mathbf{h}$ using the h_m as components.) The second type all have $E^{\bar{I}} = \varepsilon$. If the eigenvectors of type X ($=I$ or $\bar{I}$) are taken to be of the form

$$|\psi^X\rangle = \chi^X |0\rangle + \sum_{m=1}^{M} \psi_m^X |m\rangle , \tag{3.3}$$

then the eigenvectors corresponding to the above eigenvalues are determined by (defining $\boldsymbol{\psi}$ using the components ψ_m)

$$\frac{\boldsymbol{\psi}^I}{\chi^I} = \frac{\mathbf{h}}{E_I - \varepsilon} , \tag{3.4}$$

$$\mathbf{h}^* \cdot \boldsymbol{\psi}^{\bar{I}} = 0, \quad \chi^{\bar{I}} = 0 . \tag{3.5}$$

This may be interpreted geometrically: the eigenvectors which have their energies changed by the coupling have $\boldsymbol{\psi} \propto \pm \mathbf{h}$ (3.4) (and will be called "parallel" from now on) while the unshifted eigenvectors have $\boldsymbol{\psi} \perp \mathbf{h}^*$ (3.5) (called "perpendicular"). A very important point, in the light of what will follow, is that this simple result is destroyed if the site energies (of the noncentral sites) are different. Then, the best that can be achieved is to group the noncentral sites into sets with degenerate site energies and apply the result to each group in turn. Finally, note that, in general, $\boldsymbol{\psi}$ may be a complex vector, for instance, in the case where all h_m are equal, then the components of $\boldsymbol{\psi}$ can be chosen as the powers of the Mth roots of unity.

The above result will be used on various subgraphs of the graph of the Hamiltonian, with the aim of reducing the entire problem to a simple TBS form. The first application of the result is to generate a convenient initial basis for the treatment of the Hamiltonian (2.6). (This is treated more fully in our paper.[7]) Consider removing the $\mathbf{k}$-dependent links in the graph in Fig. 1: then we are left with a Cayley tree. In that case, repeated use of the above results[7] to each node in the graph produced a hierarchical solution, with the "χ" being a member of the set of "ψ_m" associated with the nodes of the *previous* generation. The hopping terms are all identical in this case, so we may use the remark at the end of the last paragraph. Thus, we find a basis set $\{|n;\{\boldsymbol{\alpha}\};\mathbf{k}\rangle\}$, where the set of conjugate variables to the sibling numbers, $\{\mathbf{i}\}$, the "sibling momenta," are $\{\alpha_i : 0 \le i \le n\} \equiv \boldsymbol{\alpha}$. Explicitly,

$$|n;\{\boldsymbol{\alpha}\};\mathbf{k}\rangle = \frac{1}{\sqrt{S_n}} \sum_{\{\mathbf{i}\}} \cdots \omega_{i_m}^{\alpha_m} \cdots |n;\{\mathbf{i}\};\mathbf{k}\rangle , \tag{3.6}$$

Here, each member of the product of the powers of ω's [$\omega_{i_n} = \exp(2\pi i/\xi_n^2)$ are the appropriate roots of unity] corresponds to the set of α's for that level in the hierarchy. We have defined the normalization, $S_n = Z(Z-1)^n$ for $n \ge 0$ and $S_{-1} = 1$. Expressed in terms of the new basis states, the Hamiltonian is given by

$$\mathcal{H} = -\sum_{n\{|\alpha||\beta|\}\mathbf{k}} \xi_{n+1} (|n;\{\boldsymbol{\alpha}\};\mathbf{k}\rangle\langle n+1;\{\boldsymbol{\beta},\beta_{n+1}=0\};\mathbf{k}| + \text{H.c.}) + \sum_{n\{\alpha\}\mathbf{k}} V_n |n;\{\boldsymbol{\alpha}\};\mathbf{k}\rangle\langle n;\{\boldsymbol{\alpha}\};\mathbf{k}| + \frac{\alpha\tau}{2} \sum_{\{\alpha\}\mathbf{k}} (\mathcal{C}_{\{\alpha\}} |-1;0;\mathbf{k}\rangle\langle 1;\{\boldsymbol{\alpha}\};\mathbf{k}| + \text{H.c.}) , \tag{3.7}$$

where the structure factors are given by

$$\mathcal{C}_{\{\alpha\}} = \frac{1}{\sqrt{S_{-1} S_1}} \sum_{\{\mathbf{i}\}}^{i_1} e^{i\mathbf{k}\cdot\{\mathbf{i}\}} \cdots \omega_{i_m}^{\alpha_m} \cdots . \tag{3.8}$$

The Hamiltonian is represented by the graph in Fig. 2. The effect of the transformation when applied to the Cayley tree was to disconnect a one-dimensional branch of the lattice in "momentum" space. However, here, since the states at the second generation are connected back to the central site, the transformation leaves the graph in one connected piece. The benefit of the transformation is that the graph is more like a TBS—it has only a single loop instead of twelve.

For the sake of clarity, we will not perform the manipulations explicitly in terms of algebra for the rest of this section, but merely operate on the graph and quote the final result. The graph has three distinct components: a triangular loop, eight single legs, and three double legs. We wish to turn this structure into one where we may ap-

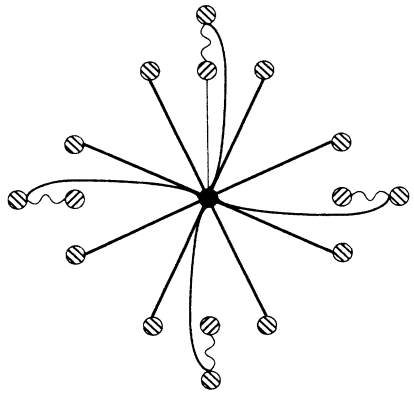

FIG. 2. The graph of the transformed Hamiltonian showing the internal separation of the tree structure. The off-diagonal matrix elements which are momentum dependent are denoted by bold lines and those which have the same value are denoted by wiggly lines. Nodes with the same "on-site" energy are shaded in the same way.

ply the TBS result directly. We may already do that to the eight single legs, which have degenerate site energies. To be able to apply it to the other two elements, we must diagonalize the 2×2 matrices corresponding to the links shown by wiggly lines in Fig. 2 present on the double-leg component and the "cross link" in the triangular loop. The resulting "bonding" and "anti-bonding" states are each connected to the central site in Fig. 2, but not to each other. The resulting graph is shown in Fig. 3(a). It is important to realize that the hopping integrals associated with the wiggly links in Fig. 2 are all the same and that the site energies at the end of the links are the same from link to link: this implies that the site energies of the legs resulting from the bonding states associated with *both* the triangle and the double legs are degenerate, and similarly for the antibonding states.

Thus, we now have a TBS with a central site and two groups of four degenerate legs and one group of eight degenerate legs. We may now form the perpendicular states associated with each of these sets independently using the result (3.5) (remember that the difference of the hopping terms within a group does not affect this result), leaving us with the diagonalization of the 4×4 matrix represented in Fig. 3(b). Although this looks like a TBS, the site energies of the legs are different and we must diagonalize this problem directly.

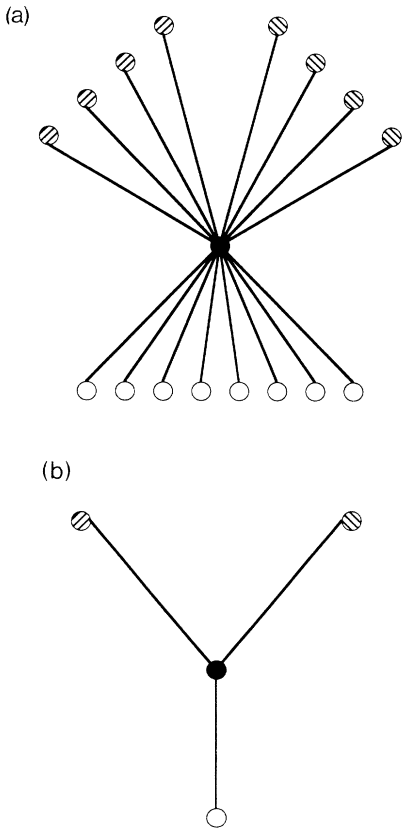

FIG. 3. (a) The graph of the Hamiltonian when transformed to a "tight-binding star." (b) The resulting connectivity of the "parallel" states after the TBS transformation. All the off-diagonal matrix elements are momentum dependent and nodes with the same "on-site" energy are shaded in the same way.

We can now see why there are only four dispersing bands: since all of the $\mathbf{k}$ dependent links emanate from the central site, and hence are not involved in determining the energies of the perpendicular states, we are only left with dispersion in states derived from three parallel states attached to the central state.

The nondispersive bands fall into two classes, which lead to states at three energies. Firstly, there are seven degenerate states which are nonbonding corresponding to the perpendicular combination of the states associated with the single legs of Fig. 2 (i.e., the second generation) having an energy

$$\varepsilon = V_1 \ . \tag{3.9}$$

Secondly, there are the three (degenerate) bonding and three (degenerate) antibonding combinations of states which are perpendicular states from the triangle and double legs (i.e., from the first and second generation) having energies

$$\varepsilon = \frac{V_0+V_1}{2} \pm \left[\frac{(V_0-V_1)^2}{4} + \xi_1^2 \right]^{1/2} \ . \tag{3.10}$$

The characteristic equation for the spectrum of the dispersive states is shown in (A15). The form of the dispersion is found to depend only on the structure factor, $\phi(\mathbf{k})$, defined in Appendix A. When the coordination number Z is four, relevant to the two-dimensional case, $\phi(\mathbf{k})$ is given by

$$\phi(\mathbf{k}) = \frac{1}{3}\left[4\cos^2\left[\frac{k_1\tilde{a}}{2}\right]\cos^2\left[\frac{k_2\tilde{a}}{2}\right] - 1 \right] \ . \tag{3.11}$$

The form of the structure factor is natural: it is derived from the sum over all the second-generation paths that allow hopping between sublattice sites. Numerical calculations indicate no band crossing of the dispersive bands as the string tension τ is varied. The complete band structure for $\tau=0.2$ and depicting all the bands is shown in Fig. 4.

When the dimensionality of the system diverges, the $\mathbf{k}$ dependence vanishes and the states become nondispersive. A hole introduced into such a system becomes localized in a quasiparticle. The energy of the quasiparticle states scale as $Z\tau$. In the next section we will discuss the behavior of the dispersive states for the two-dimensional case and focus on the lowest band in various limiting regimes.

IV. THE LOWEST BAND

So far we have been dealing with a single quasiparticle. In this section we determine the role of the calculations when there is a finite density of holes and focus on those aspects which are useful then. The first point to note is that we cannot merely "fill up" the bands to an arbitrary Fermi level: the states are many body in nature as illustrated by the number of states. However, we *can* treat the states in an approximately single-particle manner if the holes are sufficiently dilute. A crude estimate of the density, n_c, at which a gas of polarons is not a useful

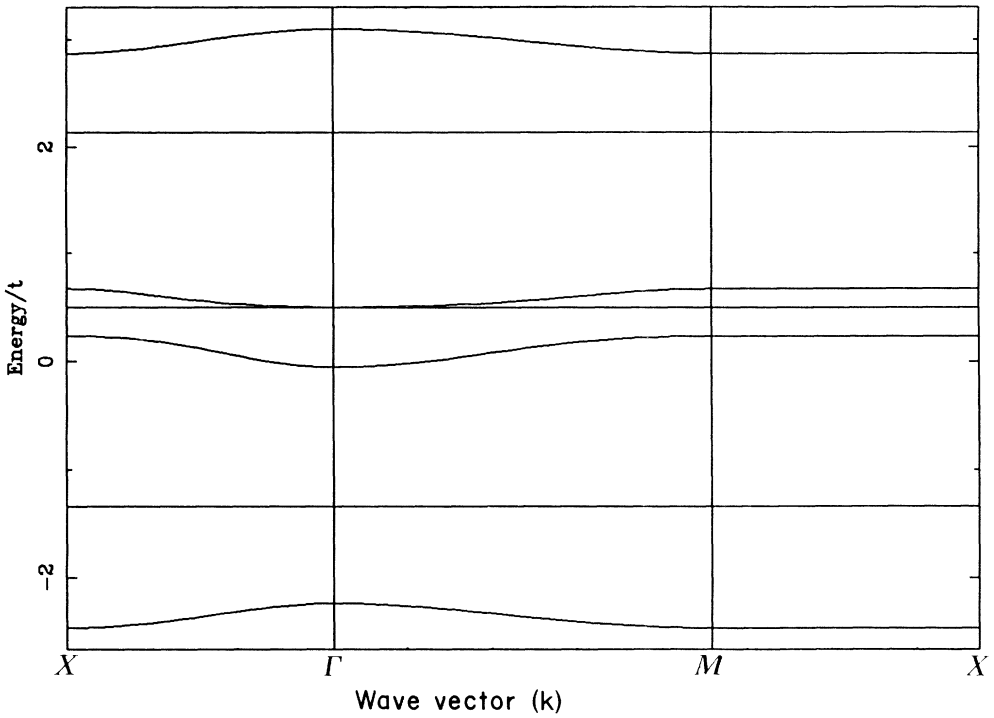

FIG. 4. The full quasiparticle band structure when $\tau=0.2$. Note that Γ, $\mathbf{k}=(0,0)$; X, $\mathbf{k}=(\pi/\bar{a},0)$; and M, $\mathbf{k}=(\pi/\bar{a},\pi/\bar{a})$, where $\bar{a}$ is the magnetic unit-cell parameter.

starting point is $n_c^{-1/d} \lesssim \xi$, where ξ is the "size" of the polaron. (In the context of the moderate to strong string tensions considered in this work, $\xi \leq 5$ lattice parameters.) The numerical work mentioned at the end of the last section implies that the dispersive bands never overlap. Thus, as the density is increased, the Fermi energy rises in the lowest band reaching n_c before any higher quasiparticle bands are occupied. Thus, ground-state properties (for $n \lesssim n_c$) are determined primarily by the lowest band, although excitations may probe the other bands.

Since one aim of the present work is partly to act as a basis for investigating Fermi-surface instabilities (either magnetic or superconducting) of the quasiparticles, we will focus, for the rest of this section, on the lowest band. We will determine both the form of the dispersion relation (and, hence effective mass) and the wave function of the quasiparticle, seeing how its "shape" distorts as $\mathbf{k}$ is varied.

Although the limit of large string tension, $\tau \gg 1$, is unphysical in the sense that it departs from the parameter space in which t-J model becomes a reliable representation of the Hubbard model, it is useful to investigate this limit to enable some interpolation across the range of string tensions. We will consider this limit first since the nature of the ground state may be readily understood.

In this limit, the hole bandwidth is constrained by the requirement that the hole must move two lattice spacings before the superexchange can operate. Consequently, the bands become dispersionless even at leading order (τ^0). In fact, the bandwidth, normalized by the energy of the hopping integral, scales like $1/\tau$. At leading order, the ground-state energy is determined purely by the energy gained from hybridizing states of the zeroth and second generations through the superexchange.

$$\varepsilon=\frac{5\tau}{4}\left[1-\left[1+\frac{48\alpha^2}{25}\right]^{1/2}\right]+O\left[\frac{1}{\tau}\right] . \tag{4.1}$$

The total energy decreases in proportion to the string tension.

The limit of greater interest is $\tau \lesssim 1$. As mentioned previously, we expect our basis set will be sufficient until $\tau \sim 0.1$. We may then *formally* exploit τ as a small parameter in determining the energy spectrum. In reality, even if $\tau=0$, there will be dispersion due to Trugman's mechanism. However, for $\tau \gtrsim 0.1$ we expect that the transverse coupling will be a more powerful agent for removing the translational degeneracy than Trugman cycles, due to the dilute nature of the latter. Thus, we assume that the expansion to leading order in the string tension τ will provide a good estimate of the dispersion of the lowest band, within the domain of validity of our variational assumptions ($\tau \gtrsim 0.1$).

Of the four dispersive bands, only three of the states are dispersive at first order in τ. In particular, the energy spectra of the lowest band is given by the following:

$$\varepsilon(\mathbf{k})=-\sqrt{7}+\frac{6\tau}{7}\left[\tfrac{3}{2}+\alpha\phi(\mathbf{k})\right]+O(\tau^2) . \tag{4.2}$$

The separation in the true energy between the lowest band and the states of the higher bands scales like t. The bandwidth of the lowest band is given by $\frac{8}{7}\alpha J$ to leading order in τ, which may be simply understood since the ma-

trix elements that lead to the delocalization are of order αJ. (The second dispersive band has twice this bandwidth.) Moreover, since the sign of the matrix elements are positive, reflecting the antiferromagnetic nature of the spin interaction, the ground state is located at the magnetic zone boundary. This result is ubiquitous amongst the numerical calculations.[8,19,20]

The ground-state energy can be more readily understood by separating the contributions from the kinetic energy, the transverse exchange energy, and the potential energy arising from the string treating the string tension τ as a small parameter.

Firstly, we find that there is no contribution to the kinetic energy arising from terms at first order in τ: the total contribution comes from the internal energy of the quasiparticle as though it were localized. Numerical simulations on 4×4 clusters[20] show a kinetic energy which varies smoothly from $-3.2t$ in the $\tau\rightarrow0$ limit to $-2.45t$ at $\tau=1$, comparing favorably with a value of $-\sqrt{7}t$ obtained from our results to leading order in τ. Allowing for the fact that in the weak string tension limit, where the quasiparticle would become extended over a wider configuration space than that chosen here, the agreement is quite good. The kinetic energy is found significantly higher than that found in the retraceable path approximation[6] of $-2\sqrt{3}t$ illustrating the difference between the two approximations.

Secondly, the contribution from the Ising exchange due to the hole-induced spin disorder is $9J/7$ which corresponds to the breaking of ca. five bonds. Again this compares favorably with the numerical simulation where they find ca. six bonds broken for most values of τ apart from the weak string tension limit where the energy seems to diverge.

The final contribution comes from the transverse exchange and is $-(2/7)\alpha J$, almost an order of magnitude smaller than the Ising contribution. This reflects the low amplitude of the wave function at the second generation which leads to the narrow bandwidth.

The bandwidth is small in both the limits $\tau\rightarrow0$ (as the matrix elements between neighboring sublattice sites are proportional to τ) and $\tau\rightarrow\infty$ (as then the hole is confined to the lowest generation by the high string tension). Therefore, it is not surprising that numerically we find a maximum bandwidth of ca. $0.8t$ when τ is of the order unity (Fig. 5). The shape of the bands is entirely determined by the structure factor. Examination of the structure factor shows that the bands only disperse *normal* to the faces of the magnetic zone, thus the Fermi surface has the normal "television screen" shape of a square with rounded-off corners. The effective one-dimensionality of the band structure implies an effective mass divergent at the magnetic zone boundary and very anisotropic.

The wave function for states of the lowest band have been calculated explicitly for both limits of the string tension, discussed above, in Appendix B. The behavior of the wave function is again complicated by the competition arising from the localizing (Ising) potential and the matrix element controlling the bandwidth both scaling with the exchange constant. When the string tension is both divergent and vanishing, approximately one-fifth of the amplitude of the wave function resides at the outer generation. The proportion changes only marginally as the string tension explores intermediate values. This reflects the effective cancellation of the two effects discussed above. The relative amplitude of the first and

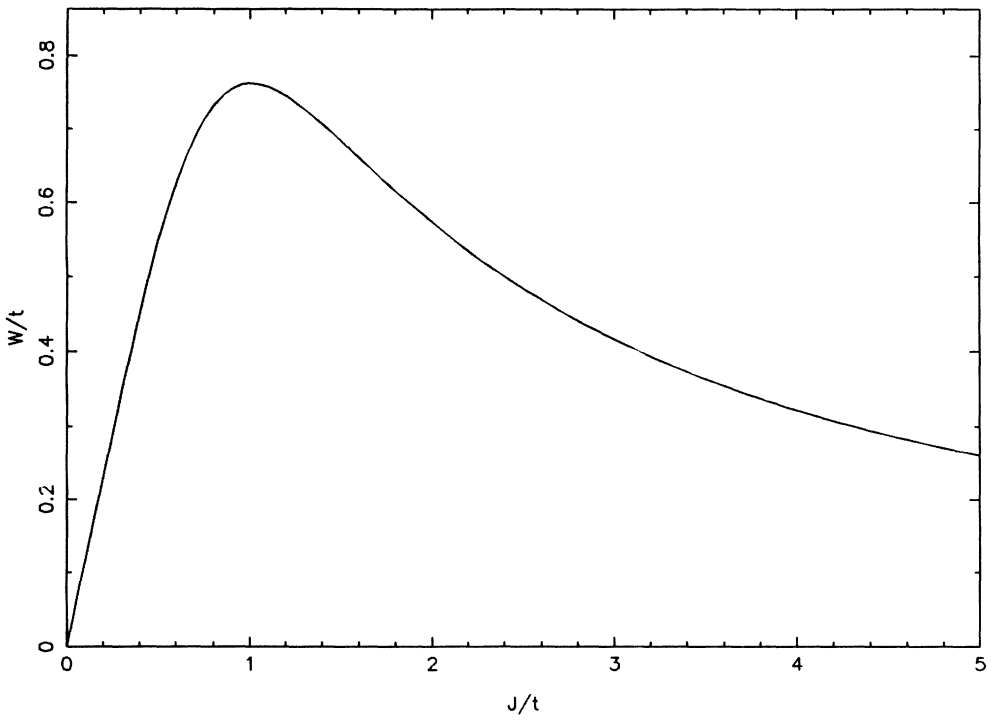

FIG. 5. The bandwidth W of the lowest band as a function of the string tension τ.

second generation account for the largest fluctuation as the string tension is varied. Firstly, since states of the first generation can only be accessed through hole motion, and not the spin dynamics alone, the increase in Ising energy causes the amplitude at this generation to vanish with increasing string tension. However, in the limit in which τ vanishes, and the problem merely resembles a tight-binding Cayley tree, the amplitude at the first generation rises to one-half.

The spin dynamics also causes an anisotropy of the wave function. The nature of this anisotropy depends on the quasiparticle momentum. At the zone boundary the matrix element which connects the central generation to the outer generations is negative, and hence favors an increase in the second-generation amplitude over the Ising limit. Clearly this tendency is at a maximum when the matrix elements are negative in *both* directions—that is, when motion is parallel to the sublattice axes. If this is not the case, then there is an anisotropy caused by the preferential increase in amplitude in the direction of motion. Conversely, at the zone center there is no anisotropy and the amplitude on the second generation is diminished, as compared to the Ising limit (as the matrix element is positive).

V. SPIN DISTORTION AROUND A HOLE

In this section we investigate the local spin distortion induced by a hole. Specifically we examine the ability of the hole to drive neighboring spins towards a relative singlet or triplet configuration as a function of quasiparticle momentum by determining the change in the expectation value of the total spin on introducing a single hole into the antiferromagnetic background. Since our approximation does not start with the true total spin-singlet antiferromagnetic ground state, it is sensible to discuss only the change in the expectation value of the total spin and not the absolute calculated value.

The total spin of the system is defined by the following operator:

$$\hat{\mathbf{S}}^2=\left[\sum_l \mathbf{S}_l\right]^2 . \tag{5.1}$$

For the rest of this section, when referring to the total spin of a given state, we will implicitly refer to the expectation value of this operator. Since the hole quasiparticle states are defined in terms of hole trajectories on a Néel background, it is helpful to determine the total spin of the original state. The Néel state may be described by $\mathcal{N}$ magnetic unit cells each with an up and a down spin. We will first focus on the "off-diagonal" part of the operator between the spins on two *different* magnetic cells. Since there is no "in-plane" component to the individual spins, the contribution from the transverse components of the operator is zero. Furthermore, since there are two antiparallel spins in each cell, the Ising contribution also vanishes. The net contribution arises from the diagonal contribution alone. Summing the "on-site" spin, $2\times\frac{3}{4}$, and the cross terms, $2\times-\frac{1}{4}$, the total spin of the Néel state is found to be the following:

$$\langle \text{Néel}|\hat{\mathbf{S}}^2|\text{Néel}\rangle=\mathcal{N} . \tag{5.2}$$

The rest of the section is concerned with determining the manner in which the total spin of the system changes when a single hole is introduced in the half-filled state. It is natural, therefore, to first examine the total spin of a state in which a single hole is *fixed* in a Néel-ordered background.

Again, since the off-diagonal part of the sum vanishes, the correction due to the hole simply arises from the diagonal contribution at the cell in which the hole resides, $-\frac{3}{4}$ from the missing spin and $2\times\frac{1}{4}$ from the Ising contribution lost. The total spin of the state is therefore, $\mathcal{N}-\frac{1}{4}$.

In fact, it is simple to deduce the total spin of the state created when the hole is allowed to wander along some trajectory. Since, the operator which measures the total spin calculates the scalar product of all spins with all other spins, any hole trajectory is guaranteed to give a state with the same total spin as the hole fixed in a Néel background. It is only by constructing a state in which the spins are allowed to develop transverse components that the total spin can change.

The average spin on a site does not change in direction in the presence of a hole quasiparticle, as this requires the hole motion to mix in the state where the spin of interest is inverted *with all other spins unaltered* and the hole is in the same position. This cannot happen as it does not conserve total S^z. However, the net spin of *near neighbors* is allowed to change in direction. In fact, there is a tendency of neighboring spins to be driven towards a singlet or triplet state depending on the relative phase of string configurations on neighboring sublattice sites. The superposition of a string configuration of length two from one sublattice site having its associated hole sharing the same site as a string configuration of zero length on a neighboring sublattice site superposes an "up-down" spin pair with a "down-up." At the zone center these states sum with equal phase tending towards a triplet whereas, at the magnetic zone boundary, we expect that they sum with opposite phases tending towards a singlet. The truncation of the basis set at a maximum string length of two implies that this scenario is the only one in which a transverse component can develop. The total spin of the hole quasiparticle state is therefore determined by the Ising contribution, which assumes the static hole value together with the transverse contribution:

$$\langle \psi(\mathbf{k})|\hat{\mathbf{S}}^2|\psi(\mathbf{k})\rangle=\mathcal{N}-\tfrac{1}{4}+2\sum_{\hat{\mathbf{e}}_l}\mathcal{C}_{\perp\hat{\mathbf{e}}_l}(\mathbf{k}) , \tag{5.3}$$

where the correlation function $\mathcal{C}_{\perp\hat{\mathbf{e}}_l}(\mathbf{k})$ can either be written in terms of spin operators or in terms of the string basis states:

$$\begin{aligned}\mathcal{C}_{\perp\hat{\mathbf{e}}_l}(\mathbf{k})&=\sum_i \tfrac{1}{2}\langle S_i^+ S_{i+\hat{\mathbf{e}}_l}^- + S_i^- S_{i+\hat{\mathbf{e}}_l}^+\rangle ,\\ &=\sum_{\mathbf{k}\{i\}} \tfrac{1}{2}\langle e^{-i\mathbf{k}\cdot|\mathbf{i}|}|-1;\mathbf{k}\rangle\langle 1;\{\mathbf{i}\};\mathbf{k}| + \text{H.c.}\rangle\end{aligned} \tag{5.4}$$

Although the correlation function enters the total spin as an invariant sum along all four lattice directions, it is interesting to focus on a particular component and thereby demonstrate the anisotropy of the spin distortion of neighboring spins. The symmetry of the correlation function is determined by

$$\sin(k_1\tilde{a})\sin(k_2\tilde{a}) \sim \cos(2k_x a) - \cos(2k_y a) \ . \tag{5.5}$$

The correlation function, therefore, displays reflection symmetry about the x and y directions together with symmetry under inversion. The anisotropy, which vanishes at both the zone center and the magnetic zone boundary, enchances the degree to which the neighboring spins are driven towards a singlet configuration along the direction of motion as the momentum approaches the magnetic zone boundary. The enhancement along the direction of motion is exactly cancelled by the diminution perpendicular to the direction of motion disguising this effect in the invariant sum.

The tendency to form singlets at the magnetic zone boundary (at least at symmetry points) and triplets at the zone center is shown by the spin distortion induced by the special class of hole motions (discovered by Trugman[8]) which allow the hole to hop one sublattice parameter, while leaving the final spin arrangement still Néel-like.

The total spin, calculated to leading order in the string tension, is given by the following:

$$\langle \psi(\mathbf{k}) | \hat{\mathbf{S}}^2 | \psi(\mathbf{k}) \rangle = \mathcal{N} - \tfrac{1}{4} + \frac{6}{7} \left[2\phi(\mathbf{k}) - \frac{\tau}{7\sqrt{7}} [35\alpha + 2(1+7\alpha)\phi(\mathbf{k}) - 36\alpha\phi(\mathbf{k})^2] \right] . \tag{5.6}$$

This shows that, when the string tension is small, there is a tendency to drive the system towards a state of low spin at the magnetic zone boundary and high spin at the zone center. In fact, the latter tendency becomes reversed in the limit of high string tension when the states of zero momentum drive the system towards a state of low spin even more vigorously than at the magnetic zone boundary.

VI. DISCUSSION

There are two striking aspects of the results of this work: the singlet nature of the spin distortion for low-energy quasiparticles (which reside at the zone boundary) and the preponderance of flat bands when hopping is included. We will now discuss these in turn.

The singlet nature of the quasiparticles is counterintuitive in the light of the Nagaoka[5] result which shows the ground state to be ferromagnetic in the zero superexchange limit: it might be expected that the ferromagnetism remained within the bounds of a spin polaron when the superexchange was included. There are really separate reasons for the occurrence of singlet tendencies and absence of ferromagnetism. The *Heisenberg* superexchange causes the quasiparticles to reside at the zone boundary (*not* the zone center as in the case of the Nagaoka state); this changes the phase of the superposition of the spin configurations—as discussed in the last section. It is interesting to note that the tendency of a single hole to drive the spin system towards a singlet is in accordance with the paramagnetic nature of the superconducting phase of the cuprates. It is tempting to ascribe the absence of ferromagnetism to the size of our basis set: it is not large enough to allow spin configurations to be superposed by the hole motion *alone* and hence the Nagaoka mechanism to work. However, it seems clear that this requires the hole-hopping integral to be substantially larger than the superexchange, so that the string of displaced spins does not dissolve under the influence of the superexchange before the hole has completed a loop. We suspect that the real case of the Cu-O planes corresponds to the regime where the Nagaoka effects are not predominant.

Another notable feature of the results is the existence of many dispersionless bands present in the quasiparticle band structure. Although we would expect the inclusion of higher-order string states and Trugman cycles to cause a small amount of dispersion to develop in these bands the bandwidth would still remain much less than the bare bandwidth of the hole.

The predominance of flat bands mirrors the recent angle-resolved photoemission data on single crystals of both the Bi-(Refs. 21-23) and Y-based[24] superconducting cuprates where several flat, excited quasiparticle bands were found, in disagreement with single-particle calculations. We would interpret these bands as being of an *inherent* many-particle nature, corresponding to excitations of the spin distortion of the short-range Néel order around the hole. It is tempting to make a more detailed fit of the data to the parameters in the model when we find that, in the case of the experiments performed on $Bi_2CaSr_2Cu_2O_8$ by Takahasi *et al.*,[21,22] a choice of $J=0.15$ eV and $J/t=0.6$ gives an almost perfect overlap. These experiments remain rather controversial and the fit may be fortuitous. Nevertheless, it demonstrates the ability of the model to reproduce the observed features at the correct energy scales.

Why are there so many flat bands? Equivalently, why is it so easy to establish spin distortions, centered on one unit cell, which have no matrix elements to a neighboring cell? It seems difficult to answer this in an entirely satisfactory manner: fundamentally it is the lack of loops in the configuration space of the hole and spins. More explicitly, the topology of the graph of the Hamiltonian, depicted in Fig. 1, is rather ramified and this facilitates composing superpositions (of configurations) which have no amplitude at the $\mathbf{k}$-dependnent links.

The sufficiency of our approximation (the truncated basis set) depends on the appropriate ratio of J/t: as long as this ratio is larger than ca. 0.1, the treatment there should be adequate. Supporting evidence for this view comes from various numerical calculations of the spectral function of a hole in the t-J model on a 4×4 lattice.[4,13,20,25] A sharp quasiparticle peak is observed with an energy scaling like the Ising hole quasiparticle. The quasiparticle is attributed to the remnants of the Ising

string polaron in the Heisenberg limit.

In conclusion, we have demonstrated that hole quasiparticles in a Néel state reside in polaronic states. These are associated with induced singlets on neighboring spins, *not* with local Nagaoka ferromagnetic tendencies. They have internal excited states most of which are dispersionless, in qualitative agreement with photoemission results. We have discussed the anisotropy of the amplitude of the quasiparticle and the associated spin distortion in the Brillouin zone.

ACKNOWLEDGMENTS

We would like to thank M.W. Long for numerous and fruitful discussions.

APPENDIX A

Determining the ground-state wave function is complicated by the excessive algebra and as such is presented in this appendix. Since our aim is to establish the lowest-energy band, we depart a little from the prescription given in the text in order to minimize the total number of basis states. Finally, we will display the wave function of the lowest band calculated to leading order in the string tension, τ.

The representation of the Hamiltonian defined in terms sibling momenta is denoted by the graph in Fig. 2. Since the $\mathbf{k}$-dependent links emanate from only the central site, we can deduce that the dispersive states must be contained within the manifold of which the state at the central site is a member. By recursively operating the Hamiltonian on the states derived from the central state, this manifold of states can be generated. In fact, there are only six such states defined below. We have chosen to return to the original sibling basis in order that the wave function may be more readily related to the underlying lattice. Firstly, there are the isotropic superpositions of all the spin configuration states of a given generation. In the absence of spin dynamics these states provide the basis for the invariant wave functions:

$$
\begin{aligned}
|1,\mathbf{k}\rangle &= |-1;0;\mathbf{k}\rangle \ , \\
|2,\mathbf{k}\rangle &= |0;\alpha_0=0;\mathbf{k}\rangle \\
&= \frac{1}{\xi_0}\sum_{\{\mathbf{i}\}} |0;\{\mathbf{i}\};\mathbf{k}\rangle \ , \qquad \text{(A1)} \\
|3,\mathbf{k}\rangle &= |1;\alpha_0=0,\alpha_1=0;\mathbf{k}\rangle \\
&= \frac{1}{\xi_0\xi_1}\sum_{\{\mathbf{i}\}} |1;\{\mathbf{i}\};\mathbf{k}\rangle \ .
\end{aligned}
$$

Secondly, there are the states which incorporate a momentum dependent phase twist in the superposition of the spin-configuration states:

$$
\begin{aligned}
|4,\mathbf{k}\rangle &= \frac{1}{\Gamma_1}\sum_{\alpha}(1-\delta_{\alpha_0,0})\delta_{\alpha_1,0}\mathcal{C}^*_{\alpha}|0;\boldsymbol{\alpha};\mathbf{k}\rangle \\
&= \frac{\xi_1}{\Gamma_1}\sum_{\{\mathbf{i}\}}[\kappa_{i_0}-\phi(\mathbf{k})]|0;\{\mathbf{i}\};\mathbf{k}\rangle \ , \\
|5,\mathbf{k}\rangle &= \frac{1}{\Gamma_1}\sum_{\alpha}(1-\delta_{\alpha_0,0})\delta_{\alpha_1,0}\mathcal{C}^*_{\alpha}|1;\boldsymbol{\alpha};\mathbf{k}\rangle \\
&= \frac{1}{\Gamma_1}\sum_{\{\mathbf{i}\}}[\kappa_{i_0}-\phi(\mathbf{k})]|1;\{\mathbf{i}\};\mathbf{k}\rangle \ , \qquad \text{(A2)} \\
|6,\mathbf{k}\rangle &= \frac{1}{\Gamma_2}\sum_{\alpha}(1-\delta_{\alpha_1,0})\mathcal{C}^*_{\alpha}|1;\boldsymbol{\alpha};\mathbf{k}\rangle \\
&= \frac{1}{\Gamma_2}\sum_{\{\mathbf{i}\}}(e^{i\mathbf{k}\cdot\{\mathbf{i}\}}-\kappa_{i_0})|1;\{\mathbf{i}\};\mathbf{k}\rangle \ ,
\end{aligned}
$$

where the structure factors are given by

$$\kappa_{i_0}=\frac{1}{\xi_1^2}\sum_{\{\mathbf{j}\}}\delta_{i_0 j_0}e^{i\mathbf{k}\cdot\{\mathbf{j}\}} \qquad \text{(A3)}$$

and

$$\phi(\mathbf{k})=\frac{1}{\xi_0^2}\sum_{i_0}\kappa_{i_0} \ , \qquad \text{(A4)}$$

and the normalizations by the following:

$$\Gamma_1^2(\mathbf{k})=Z[1-\phi(\mathbf{k})][(Z-1)\phi(\mathbf{k})+1] \ , \qquad \text{(A5)}$$

$$\Gamma_2^2(\mathbf{k})=Z(Z-2)[1-\phi(\mathbf{k})] \ . \qquad \text{(A6)}$$

Before presenting the matrix elements between the six basis states it is useful to define the following structure factors:

$$\mathcal{J}_0(\mathbf{k})=\tfrac{1}{2}\alpha\tau\sqrt{Z(Z-1)}\phi(\mathbf{k}) \ , \qquad \text{(A7)}$$

$$\mathcal{J}_1(\mathbf{k})=\tfrac{1}{2}\alpha\tau\Gamma_1(\mathbf{k}) \ , \qquad \text{(A8)}$$

$$\mathcal{J}_2(\mathbf{k})=\tfrac{1}{2}\alpha\tau\Gamma_2(\mathbf{k}) \ . \qquad \text{(A9)}$$

The graph of the Hamiltonian which connects the six basis states described above is shown in Fig. 6. The matrix elements are shown in detail below:

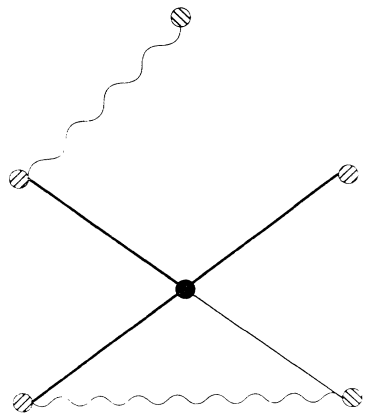

FIG. 6. Graph of Hamiltonian described in terms of the six basis states defined in Appendix A. The off-diagonal matrix elements which are momentum dependent are denoted by bold lines and those which have the same value are denoted by wiggly lines. Nodes with the same "on-site" energy share the same shading.

$$H=\begin{bmatrix} 0 & -\xi_0 & \mathcal{J}_0 & 0 & \mathcal{J}_1 & \mathcal{J}_2 \\ -\xi_0 & V_0 & -\xi_1 & 0 & 0 & 0 \\ \mathcal{J}_0 & -\xi_1 & V_1 & 0 & 0 & 0 \\ 0 & 0 & 0 & V_0 & -\xi_1 & 0 \\ \mathcal{J}_1 & 0 & 0 & -\xi_1 & V_1 & 0 \\ \mathcal{J}_2 & 0 & 0 & 0 & 0 & V_1 \end{bmatrix} . \tag{A10}$$

Notice that, at the Brillouin-zone center where the structure factors $\mathcal{J}_1$ and $\mathcal{J}_2$ vanish, the two branches which do not loop become disconnected from the central site. In fact, the detached states become undefined since they vanish in this limit. Thus, there are only three states which have a finite amplitude at the origin (this compares with the ordinary Cayley tree). These are the states which are invariant under permutations of the branches of the tree.

Furthermore, for the two-dimensional case, when $\mathcal{Z}=4$, at the magnetic zone boundary $\mathcal{J}_1$ vanishes along with the contribution of the fourth and fifth basis states to the bonding eigenstates. The anisotropy of these states is determined by the amplitude of the sixth basis state alone. This implies that the wave function for states along the boundary remains invariant at the first generation.

Although this reduced basis set contains the dispersive states, we have not eliminated all the nondispersive eigenstates which have a node on the central site. The elimination of such states is achieved by constructing the bonding and nonbonding combination of states about the **k**-independent matrix elements denoted by the wiggly lines in Fig. 6. The result of this procedure is the generation of the manifold of states which describe all four of the dispersive states. The unitary matrix which separates out the two nondispersive states is shown below, the eigenvectors of the two states occupying the first two columns:

$$U^{\dagger}=\begin{bmatrix} 0 & 0 & 1 & 0 & 0 & 0 \\ \delta_+\mathcal{N}_+ & \delta_-\mathcal{N}_- & 0 & \mu_+\delta_+\mathcal{N}_+ & \mu_-\delta_-\mathcal{N}_- & 0 \\ \mathcal{N}_+ & \mathcal{N}_- & 0 & \mu_+\mathcal{N}_+ & \mu_-\mathcal{N}_+ & 0 \\ \mu_+\delta_+\mathcal{N}_+ & \mu_-\delta_-\mathcal{N}_- & 0 & -\delta_+\mathcal{N}_+ & -\delta_-\mathcal{N}_- & 0 \\ \mu_+\mathcal{N}_+ & \mu_-\mathcal{N}_- & 0 & -\mathcal{N}_+ & -\mathcal{N}_- & 0 \\ 0 & 0 & 0 & 0 & 0 & 1 \end{bmatrix} , \tag{A11}$$

where

$$\delta_+\equiv-\frac{1}{\delta_-},\quad \delta_\pm=\left[\frac{V_1-\lambda_\pm}{V_0-\lambda_\pm}\right]^{1/2},\quad \mu_\pm=\frac{\xi_0\delta_\pm-\mathcal{J}_0}{\mathcal{J}_1},\quad \mathcal{N}_\pm^{-2}=(1+\delta_\pm^2)(1+\mu_\pm^2) . \tag{A12}$$

The eigenvalues of the nondispersive states in this reduced basis are given by the following:

$$\lambda_\pm=\frac{V_0+V_1}{2}\pm\left[\frac{(V_0-V_1)^2}{4}+\xi_1^2\right]^{1/2} . \tag{A13}$$

Finally, the matrix elements of the part of the Hamiltonian which connects the four basis states for the dispersive eigenstates are shown below:

$$H=\begin{bmatrix} 0 & -\mathcal{J}_1\left[\frac{1+\mu_+^2}{1+\delta_+^2}\right]^{1/2} & -\mathcal{J}_1\left[\frac{1+\mu_-^2}{1+\delta_-^2}\right]^{1/2} & \mathcal{J}_2 \\ -\mathcal{J}_1\left[\frac{1+\mu_+^2}{1+\delta_+^2}\right]^{1/2} & \lambda_+ & 0 & 0 \\ -\mathcal{J}_1\left[\frac{1+\mu_-^2}{1+\delta_-^2}\right]^{1/2} & 0 & \lambda_- & 0 \\ \mathcal{J}_2 & 0 & 0 & V_1 \end{bmatrix} . \tag{A14}$$

These states form a "tight-binding star" [as depicted in Fig. 3(b)] with differing matrix elements and site energies but all connected to the central site. The resulting characteristic equation which determines the eigenvalues does not yield a simple analytic solution. The precise equation is shown below for the two-dimensional case when the coordination number is four:

$$\varepsilon^4-\tfrac{13}{2}\tau\varepsilon^3+[(\tfrac{55}{4}-3\alpha^2)\tau^2-7]\varepsilon^2-(\tfrac{75}{2}\tau^2-48\alpha^2\tau^2-110+48\alpha\phi)\frac{\tau}{4}\varepsilon-[25-6\alpha^2(1-\tfrac{15}{8}\tau^2)-6(5-\alpha)\alpha\phi]\tau^2=0 . \tag{A15}$$

The solution of the quartic is discussed in the text.

When the dimensionality (and therefore the coordination number Z) diverges the $\mathbf{k}$ dependence vanishes from the problem and the energy scale of $Z\tau/2$ emerges. Remormalizing the energy by this factor is done by defining

$$\varepsilon=\frac{Z\tau}{2}\chi\ . \tag{A16}$$

The roots of the characteristic equation are then given by the following:

$$\chi=1,2,1\pm(1+\alpha^2)^{1/2}\ . \tag{A17}$$

APPENDIX B

It is useful to determine the form of the wave function in the following perturbative limits. Firstly, when the magnitude of the exchange constant becomes much less than the magnitude of the hopping integral, the hole is able to delocalize through the creation of string configurations but the net motion of the strings through superexchange is diminished. It is in the extreme limit that the truncation of the basis states becomes inadequate. Nevertheless, the strength of the localizing potential enables the justification for the higher region of the limit. Secondly, when the exchange constant becomes much larger than the hopping integral, the hole motion becomes dominated by the hopping integral since the strings very readily exchange binding sites. Since the superexchange is derived from second-order correlations induced through the same hopping integral, this limit is unphysical. Nevertheless, the interpolation between these regimes should enable a clearer understanding of the evolution of the wave function. Throughout we will assume a coordination number Z, of four relevant to the two-dimensional case.

We will first consider the limit in which τ tends to zero. The wave function may be more readily understood by considering the Hamiltonian acting on the six basis states defined by (A1) and (A2). The eigenstates of the unperturbed Hamiltonian are given by the following unitary matrix:

$$Y^{\dagger}=\begin{bmatrix} \sqrt{2/7} & \sqrt{3/7} & -\sqrt{2/7} & 0 & 0 & 0 \\ \frac{1}{\sqrt{2}} & 0 & \frac{1}{\sqrt{2}} & 0 & 0 & 0 \\ \sqrt{3/14} & -\frac{2}{\sqrt{7}} & -\sqrt{3/14} & 0 & 0 & 0 \\ 0 & 0 & 0 & \frac{1}{\sqrt{2}} & \frac{1}{\sqrt{2}} & 0 \\ 0 & 0 & 0 & \frac{1}{\sqrt{2}} & -\frac{1}{\sqrt{2}} & 0 \\ 0 & 0 & 0 & 0 & 0 & 1 \end{bmatrix}\ . \tag{B1}$$

The first three states correspond to the invariant eigenstates of the tight-binding Cayley tree of depth two. The eigenvalues are given by $-\sqrt{7}$, 0, and $\sqrt{7}$, respectively.

The effect of the perturbation is to enable the delocalization through the exchange of spins. Focusing on the lowest band of states, the energy spectrum is given by

$$-\sqrt{7}+\tfrac{3}{7}[3+2\alpha\phi(\mathbf{k})]\tau+O(\tau^2)\ , \tag{B2}$$

and the wave function by

$$|\psi,\mathbf{k}\rangle=\begin{bmatrix} \sqrt{2/7}\left[1+\frac{3}{7\sqrt{7}}[\frac{11}{4}-\frac{1}{2}\alpha\phi(\mathbf{k})]\tau\right] \\ \frac{1}{\sqrt{2}}\left[1-\frac{3}{7\sqrt{7}}[\frac{1}{4}-\alpha\phi(\mathbf{k})]\tau\right] \\ \sqrt{3/14}\left[1-\frac{1}{7\sqrt{7}}[\frac{37}{4}+5\alpha\phi(\mathbf{k})]\tau\right] \\ -\sqrt{3/14}\frac{\mathcal{J}_1(\mathbf{k})}{2} \\ -\frac{1}{\sqrt{2}}\frac{\mathcal{J}_1(\mathbf{k})}{2} \\ -\frac{1}{\sqrt{2}}\frac{2\mathcal{J}_2(\mathbf{k})}{7} \end{bmatrix}\ . \tag{B3}$$

The variation of the wave function across the zone is discussed qualitatively in the text.

The second, less physically motivated limit arises from the perturbation at order $1/\tau$. States of the first generation, which can only be accessed through hole motion, have an amplitude which vanishes at leading order. The unperturbed Hamiltonian resembles a tight-binding star between states of the second generation and the central state. For dispersion to occur, the hole must propagate two lattice spacings resulting in a band spectrum which remains dispersionless to order τ^0. The lowest band of states have an energy given by the following:

$$\varepsilon=\frac{5\tau}{4}\left[1-\left[1+\frac{48\alpha^2}{25}\right]^{1/2}\right]+O\left[\frac{1}{\tau}\right]\ , \tag{B4}$$

with the corresponding wave function, again expressed to order τ^0, given by the following:

$$|\psi,\mathbf{k}\rangle = \frac{1}{\left[\left[\varepsilon-\frac{5\tau}{2}\right]^2+3\alpha^2\tau^2\right]^{1/2}} \begin{pmatrix} \varepsilon-\frac{5\tau}{2} \\ -\frac{1}{\varepsilon-\frac{3\tau}{2}}\left[2\left[\varepsilon-\frac{5\tau}{2}\right]+3\phi(\mathbf{k})\right]\alpha\tau \\ \sqrt{3}\phi(\mathbf{k})\alpha\tau \\ -\frac{1}{\varepsilon-\frac{3\tau}{2}}\sqrt{3}\mathcal{J}_1(\mathbf{k}) \\ \mathcal{J}_1(\mathbf{k}) \\ \mathcal{J}_2(\mathbf{k}) \end{pmatrix}. \tag{B5}$$

[1]P. W. Anderson, *Frontiers and Borderlines in Many-Particle Physics, Varenna, 1987,* Proceedings of the Enrico Fermi International School of Physics, edited by J. R. Schneffer and R. A. Broglia (North-Holland, Amsterdam, 1987).

[2]F. C. Zhang and T. M. Rice, Phys. Rev. B **37**, 3759 (1988).

[3]K. A. Chao, J. Spałek, and A. M. Oleś, J. Phys. C **10**, L271 (1977).

[4]C. -X. Chen, H. -B. Schüttler, and A. J. Fedro, Phys. Rev. B **41**, 2581 (1990).

[5]Y. Nagaoka, Phys. Rev. **147**, 392 (1966).

[6]W. F. Brinkman and T. M. Rice, Phys. Rev. B **2**, 1324 (1970).

[7]B. D. Simons and J. M. F. Gunn, Phys. Rev. B **41**, 7019 (1990).

[8]S. A. Trugman, Phys. Rev. B **37**, 1579 (1988).

[9]C. M. Varma, Phys. Rev. Lett. **61**, 2713 (1988).

[10]C. L. Kane, P. A. Lee, and N. Read, Phys. Rev. B **39**, 6880 (1989).

[11]C. Gros and M. D. Johnson, Phys. Rev. B **40**, 9423 (1989).

[12]S. A. Trugman, Phys. Rev. B **41**, 892 (1990).

[13]K. J. von Szczepanski, P. Horsch, W. Stephan, and M. Ziegler, Phys. Rev. B **41**, 2017 (1990).

[14]S. Sachdev, Phys. Rev. B **39**, 12 232 (1989).

[15]B. I. Shraiman and E. D. Siggia, Phys. Rev. Lett. **61**, 467 (1988).

[16]M. J. Godfrey and J. M. F. Gunn, J. Phys. Condens. Mater. **1**, 5821 (1989).

[17]P. W. Anderson, Science **235**, 1196 (1987).

[18]T. M. Rice, Proceedings of the 9th General Conference of the Condensed Matter Division of EPS, Nice, France [Phys. Scr. **T29**, (1989)], p. 77.

[19]B. I. Shraiman and E. D. Siggia, Phys. Rev. Lett. **60**, 740 (1988).

[20]Y. Hasegawa and D. Poilblanc, Phys. Rev. B **40**, 9035 (1990).

[21]T. Takahasi, H. Matsuyama, H. Katayama-Yoshida, Y. Okabe, S. Hosoya, K. Seki, H. Fujimoto, M. Sato, and H. Inokuchi, Nature **334**, 691 (1988).

[22]T. Takahashi, H. Matsuyama, H. Katayama-Yoshida, Y. Okabe, S. Hosoya, K. Seki, H. Fujimoto, M. Sato, and H. Inokuchi, Phys. Rev. B **39**, 6636 (1989).

[23]F. Minami, T. Kimura, and S. Takekawa, Phys. Rev. B **39**, 4788 (1989).

[24]Y. Sakisaka, T. Komeda, T. Maruyama, M. Onchi, H. Kato, Y. Aiura, H. Yanashima, T. Terashima, Y. Bando, K. Iijima, K. Yamamoto, and K. Hirata, Phys. Rev. B **39**, 9080 (1989).

[25]E. Dagotto, A. Moreo, R. Joynt, S. Bacci, and E. Gagliano, Phys. Rev. B **41**, 2585 (1990).